*J. Univ. Kuwait (Sci.)* **9**, 1982

# Lherzolite xenoliths from the Shihan basalts, Jordan

MOHAMED A. EL-SHARKAWI*

*Department of Geology, University of Kuwait*

## ABSTRACT

Fresh spinel-lherzolite xenoliths were found in the Quaternary alkaline olivine basalts from Shihan Volcanic Cone, central Jordan. Mineralogically, they consist of forsterite, Fe-enstatite, chrome-diopside and chrome-spinel set in a protogranular texture. Two generations of these minerals can be traced. Phlogopitisation of olivine is a common feature, especially for generation I forsterite. The enclosing basalt is highly contaminated by detached mineral fragments from the xenoliths. Fissure eruption dolerites exposed in nearby areas are tholeiitic and are not the feeders for Shihan basalts. It is possible that the mono-xenoliths in Shihan basalts were derived from the upper mantle and that the central volcano type eruption accompanied transcurrent faults rather than normal faults.

## INTRODUCTION

Quaternary basaltic rocks are known to occur on the eastern side of the Dead Sea rift in Jordan (Bender 1968). Extensive basaltic sheets cover the northeastern stretch of Jordan and extend into Syria. The Jordanian basalts are the least studied volcanic rocks in the region. These rocks are usually reported on in articles dealing with hydrogeology or geomorphology.

Within the vicinity of Wadi Al-Mawjib—Wadi Al-Karak District, feeder dolerite dykes (e.g. Al-Kharaza, Fig. 1) induced contact effects on the surrounding Cretaceous rocks. The Shihan volcanic cone is located on a major fault (Fig. 1) and the basaltic sheets cover a wide stretch of land, the weathering of which is the reason for the fertility of the soil in the district.

The Quaternary age (Middle Pleistocene of Bender (1968)) was assigned owing to the presence of exotic blocks of Cretaceous, Eocene and Miocene sediments as well as artifacts. The purpose of this article is to record the presence of ultramafic xenoliths, which were possibly derived from the mantle, in some basalts close to the Gebel Shihan volcanic cone. Recently, similar ultramafic xenoliths were collected from the Gebel Aritain basaltic cone in the northeastern part of Jordan. Careful inspection of the volcanic cones in Jordan may disclose a widespread occurrence of the ultramafic xenoliths.

* Present address: Department of Geology, Faculty of Science, Cairo University, Giza, Egypt.

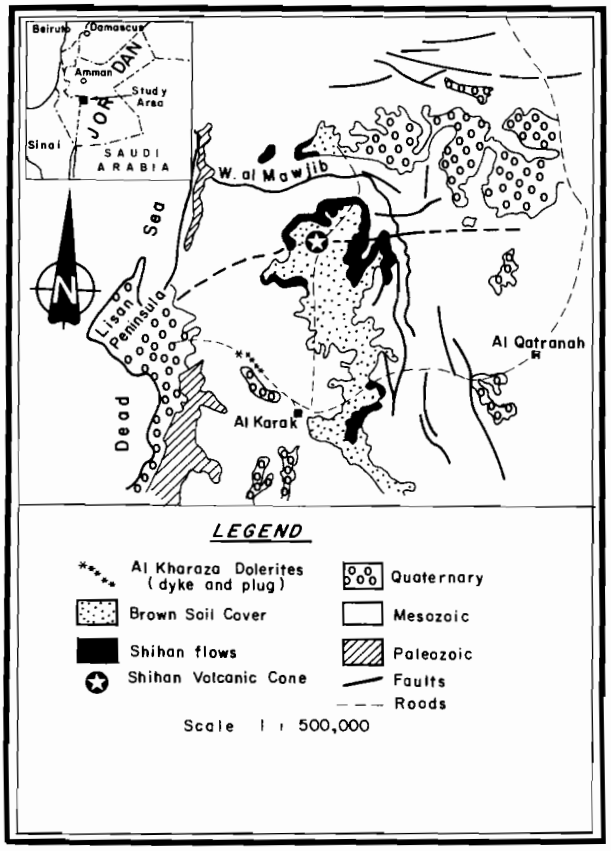


**Fig. 1.** Shihan basalts, Jordan (after Bender 1968).

## GEBEL SHIHAN VOLCANIC CONE

The Gebel Shihan volcanic cone forms a conspicuous hill, about 2 km from the Amman—Al-Karak Highway on the southern cliff of Wadi Al-Mawjib. On Bender's 1 : 100,000 map (1968) the volcanic cone is marked as Samra. It covers an area of about 25 km$^2$, and is surrounded by densely cultivated brown soil which caps the basaltic sheets (Fig. 1) exposed in Wadi Al-Mawjib. A thin veneer of brown soil caps the volcanic cone and the basaltic boulders. Unfortunately, the cone which is the highest landmark in the area was used as a fortress by the Turks and its geology is partly concealed.

It is apparent from the available geological map (Fig. 1) that the Shihan volcano erupted along a major E–W trending fault which swings in a southwesterly direction on approaching the Dead Sea rift. This fault is the western extension of the Swaqa normal fault (Hatcher *et al.* 1981).

## THE XENOLITHIC BASALTS

The presence of ultramafic xenoliths in the Shihan basalts was recognised in rolled

boulders from the Shihan volcanic cone. These were found on the slopes of Wadi Al-Mawjib close to the volcanic cone.

Basaltic rocks enclosing ultramafic xenoliths could be recognised easily in the field by the characteristically black colour of the basaltic boulders, absence of vesicles or amygdules, extreme hardness and massive nature. Occasionally, when the xenoliths occur exposed to the surface they weather easily and leave scars on the surface of the basaltic boulders (Fig. 2).

Black basalt boulders were collected from the field and sliced in the laboratory because they were difficult to break with a hammer. Apple green, fresh xenoliths of various shapes and sizes were encountered in these particular basalts. Large xenoliths range in size in the sectioned surfaces between $6{\cdot}5 \times 4{\cdot}5$ cm and $2 \times 2$ cm, while small xenoliths range between $2 \times 0{\cdot}6$ cm and $1 \times 0{\cdot}5$ cm. They are usually rounded with brownish 1–2 mm reaction margins developed toward the enclosing basalt, due to magmatic corrosion and reaction.

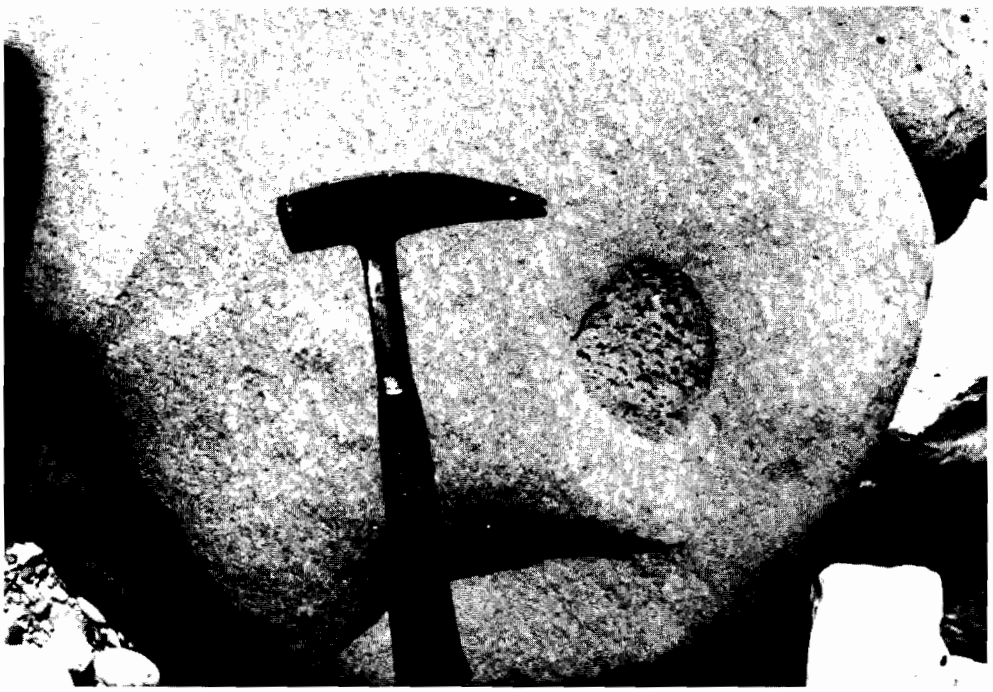

**Fig. 2.** Round ultramafic xenolith in basaltic boulder.

## PETROGRAPHY OF THE ULTRAMAFIC INCLUSIONS

The ultramafic inclusions in Shihan basaltic rocks are characteristically free of any foliation or lineation. The texture can comply with the protogranular texture of Mercier & Nicolas (1975), where the component minerals show equilibration contacts, however disturbed by the fractured nature of the minerals. Coarse grained olivine, pyroxene and spinel enclosing tiny crystals of the same minerals, are the characteristic features for these ultramafic inclusions. The modal composition of ultramafic inclusions (Table 1) showed that they can be classified as spinel-lherzolite, and are

**Table 1.** Modal composition of the lherzolite xenoliths and the enclosing basalt

A. The lherzolite xenoliths:

| Mineral | Average of three xenoliths |
|---|---|
| Olivine | 61·8 |
| Clinopyroxene (chrome diopside) | 9·0 |
| Orthopyroxene (Fe enstatite) | 26·2 |
| Spinel (chrome spinel) | 3·0 |

B. The enclosing basalt:

| Mineral | Type | Percentage | Total percentage |
|---|---|---|---|
| Olivine | Mantle xenocrysts | 3·2 | 15·8 |
| | Interstitial | 11·2 | |
| | Tecoblasts | 1·4 | |
| Plagioclase | Laths | 29·6 | 38·0 |
| | Groundmass (possibly including nepheline) | 8·4 | |
| Pyroxene (augite) | Phenocrysts | 10·0 | 26·1 |
| | Groundmass | 16·1 | |
| Magnetite | Interstitial euhedral crystals | 17·0 | 17·0 |
| Minerals in vesicles | Chalcedony, glass | 2·1 | 2·1 |

more enriched in pyroxene than those described (harzburgites) from Al-Birk area, Saudi Arabia (Ghent *et al.* 1980). The mineralogy of these xenoliths, based on textural relationships, can be assigned to two generations. Generation I (early phase of crystallisation) minerals usually occur as small crystals enclosed in larger crystals of generation II (late phase of crystallisation) minerals.

*Generation I minerals*

Early formed minerals occur as poikilitic inclusions in the coarser grained generation II minerals (Plate I, Figs 1 and 2). These minerals may be perfectly euhedral or almost rounded depending on the preservation or exposure of the generation I minerals to magmatic corrosion. Olivine is the main component of this early generation, and it suffered from deuteric alteration which resulted in the formation of phlogopite dusted with chrome-spinel. An arrested stage of phlogopitisation may be observed (Plate I, Fig. 3). Mercier & Nicolas (1975) noticed the marginal dusting of olivine crystals with spinel. Stacking of tiny olivine crystals was occasionally observed (Plate I, Fig. 4). Early formed pyroxenes were not easy to recognise, but generation I spinel

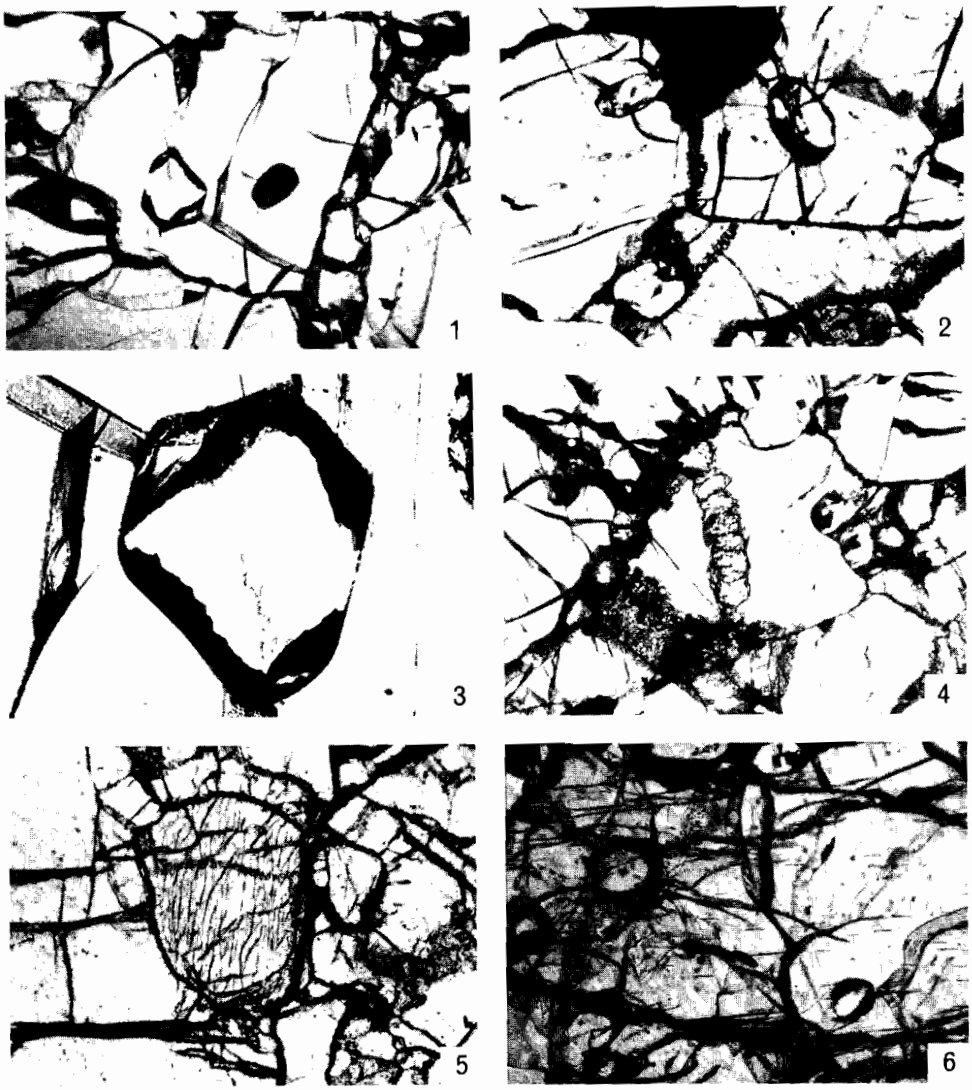


**Plate I.** The lherzolite inclusions.

**Figure**

1 Inclusions of generation I minerals in cracked olivine crystals of generation II. PPL, ×8.
2 Inclusions of euhedral and rounded crystals of generation I in olivine. Black is chrome-spinel of generation II. PPL, ×8.
3 Phlogopite, dusted with chrome-spinel, replacing euhedral generation I olivine crystal. PPL, ×32.
4 Tiny stacked generation I olivine crystals enclosed in cracked generation II olivine. PPL, ×8.
5 Clinopyroxene crystal less cracked than the surrounding olivine crystals. PPL, ×8.
6 Phlogopitised tiny olivine crystals (generation I) enclosed in cracked orthopyroxene with few exsolved lamellae. PPL, ×8.

(chrome-spinel) was easily noticed as euhedral inclusions in olivine (Plate III, Fig. 1). In some instances, olivine rims developed around the harder spinel inclusion (Plate III, Fig. 2). The rim is similar to the overgrowth or reaction rim, but it is usually incomplete. Similar features are also observed between pyroxene crystals in contact with olivine (Plate I, Fig. 5). The olivine rim is crushed and its presence may indicate stress and hence the development of incomplete crushed olivine rim against the harder spinel and pyroxene crystals.

*Generation II minerals*

In hand specimen, the minerals can be recognised according to their colours. Olivine (forsterite), the predominant mineral, is colourless, orthopyroxene (enstatite) mauve or light brown, clinopyroxene (chrome-diopside) apple green and chrome-spinel dark brown or black. The minerals are usually cracked, especially the olivine. Chrome-diopside shows well developed cleavage (Plate I, Fig. 5), and is usually strained, less cracked and has the R.I. $\beta = 1{\cdot}705$, while enstatite ($\beta = 1{\cdot}675$) is cracked and encloses tiny olivine crystals. Few unevenly distributed tiny exsolved lamellae characterise this mineral (Plate I, Fig. 6).

Most of the cracked olivine crystals ($\beta = 1{\cdot}670$) are strained and develop deformation lamellae (Plate II, Figs 1 and 2). Induced lamellar twinning is totally absent in the pyroxene. Fragmentation of olivine crystals is occasionally observed in contacts between the olivine crystals (Plate II, Fig. 2). The shattered olivine fragments were subjected to deuteric phlogopitisation (Plate III, Fig. 4). Chrome-spinel which develops interstitially to cracked olivine may be observed studded with islands of phlogopitised olivine fragments (Plate III, Fig. 3).

Chrome-spinel is dark brown ($n > 1{\cdot}90$) with black thin rims which are thought to be magnetite. The isolated grains are non-magnetic and this could be the intermediate alteration product developed during alteration of chromite (Basta & Hanafy 1970). This black margin is extensive when chrome-spinel comes in contact with the enclosing basaltic fluids or is enclosed in the basalt (see Plate IV, Fig. 5).

Generation II chrome-spinel poses some problems to be solved. It is observed petrographically that the dark colour of the phlogopite is due to the presence of spinel dust. This dust is not due to release of iron from the phlogopitised olivine (Plate III, Fig. 4). Could the formation of this generation II chrome-spinel paragenetically postdate the formation of generation II olivine, and be formed during their subsequent phlogopitisation? Remnants of phlogopitised olivine characterise generation II chrome-spinels (Plate III, Fig. 3).

Micro-seepage of basaltic fluids has occurred in some cracked olivine crystals and shows pseudo-myrmekitic pattern (Plate III, Fig. 5). In some instances acicular needles, possibly zeolite, were observed together with oriented tiny black lamellae on the surface of olivine and clinopyroxene (Plate III, Fig. 6).

## PETROGRAPHY OF THE ENCLOSING BASALT

The spinel-lherzolite xenoliths occur enclosed in a black, hard, massive, finely crystalline basalt. Details about the modal composition of this basalt are included in Table 1. The contact between the xenoliths and basalt is sharp (Plate IV, Fig. 1), but with kelyphitic rims in some instances due to magmatic corrosion. Infiltration of

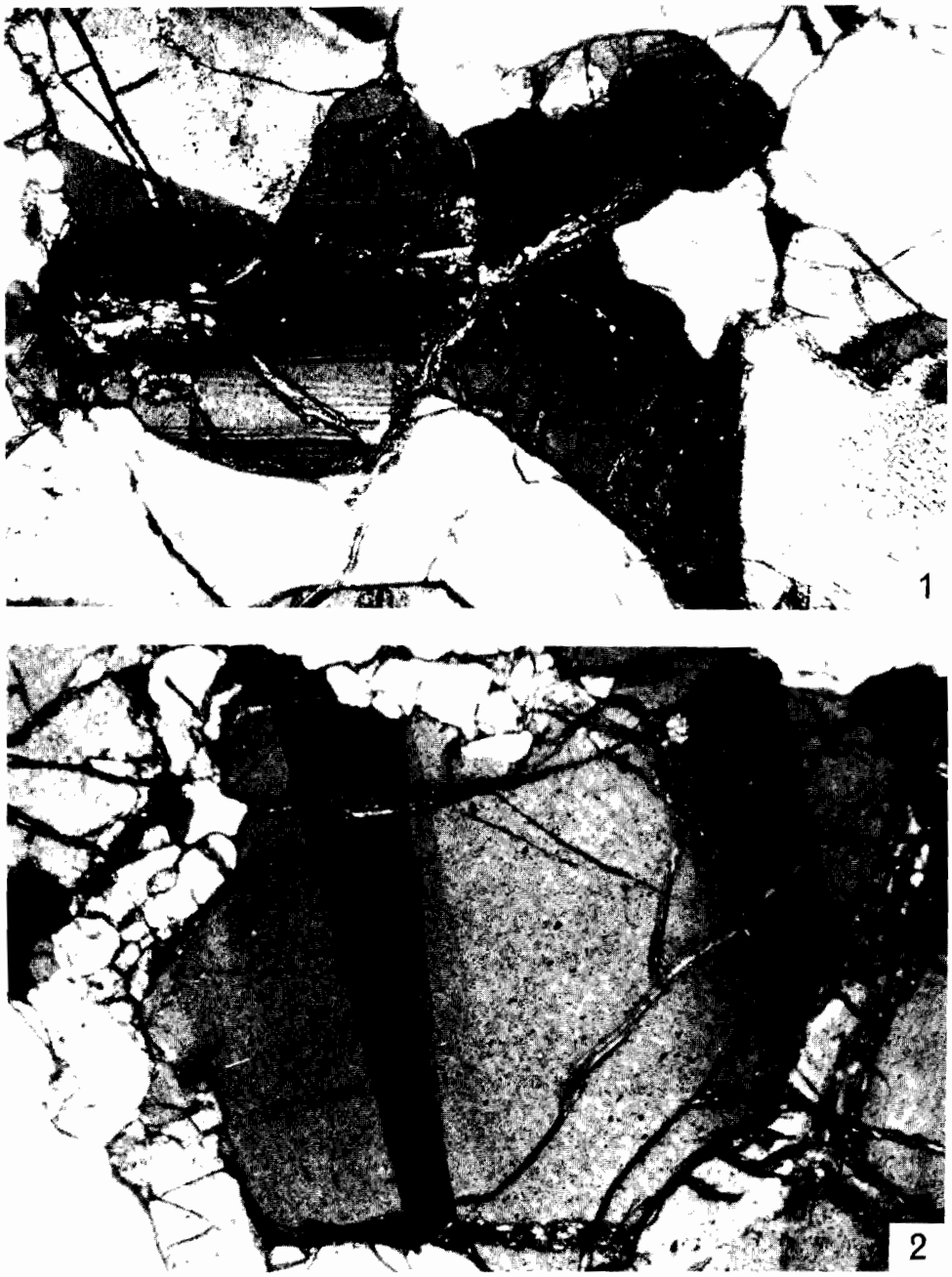


**Plate II.** Deformation lamellae in generation II olivine.

**Figure**

1 Intensively cracked olivine with curved boundary deformation lamellae. The cracks are invaded by basaltic fluids which left their trails on some crystals (lower right hand corner). Crossed polarisers, × 11.

2 Strained olivine crystal with localised deformation lamellae. A crush zone surrounds the strained crystal and consists of tiny olivine fragments. Crossed polarisers, × 11.

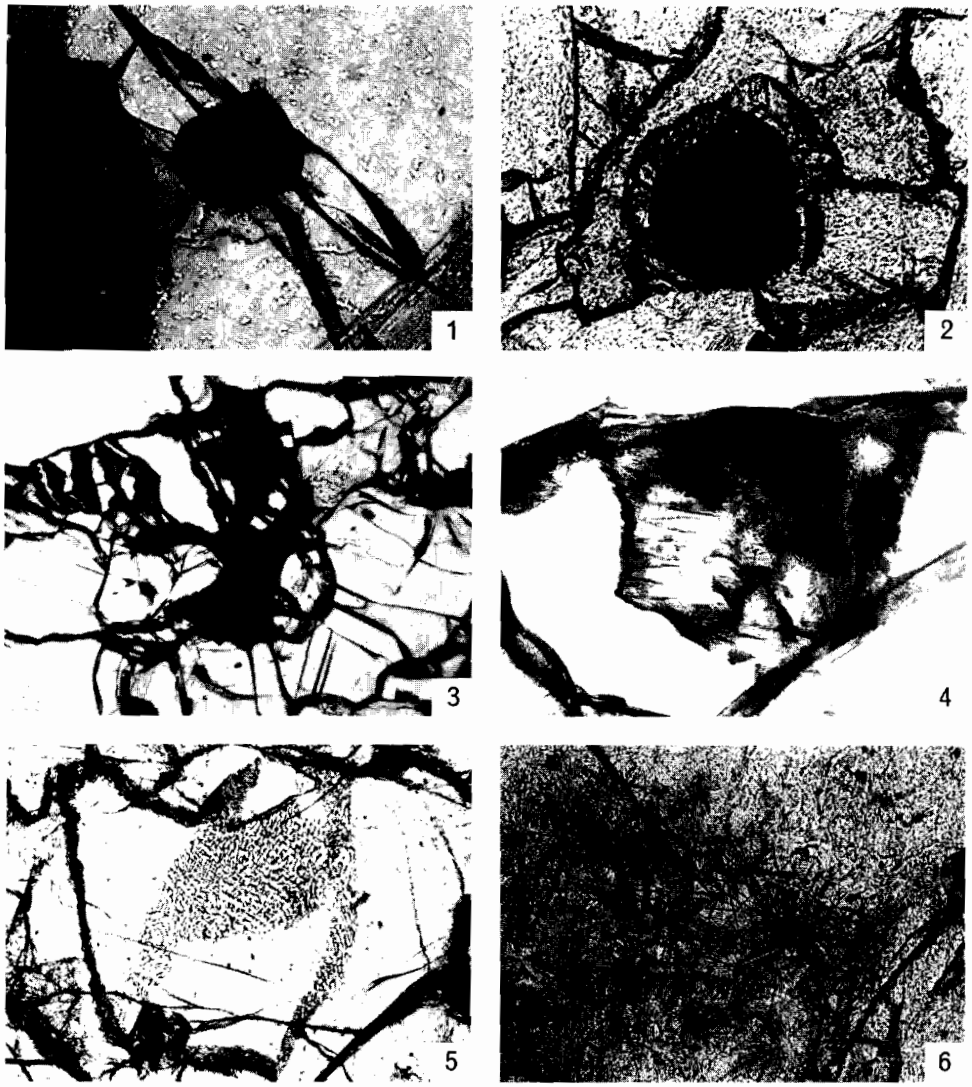


**Plate III.** The lherzolite inclusions.

**Figure**

1 Chrome-spinel euhedral crystal enclosed in cracked olivine. The black field is second generation of chrome-spinel. PPL, × 8.
2 Olivine neoform marginally developed around chrome-spinel crystal enclosed in olivine. PPL, × 8.
3 Black chrome-spinel (generation II) enclosing fragmented phlogopitised olivine. PPL, × 8.
4 Relics of olivine in chrome spinel-dusted phlogopite. PPL, × 32.
5 Trails of magmatic fluids showing pseudo-myrmekitic pattern on olivine crystal. PPL, × 10.
6 Acicular needles (zeolite?) and opaque specks oriented in clinopyroxene crystal. PPL, × 8.

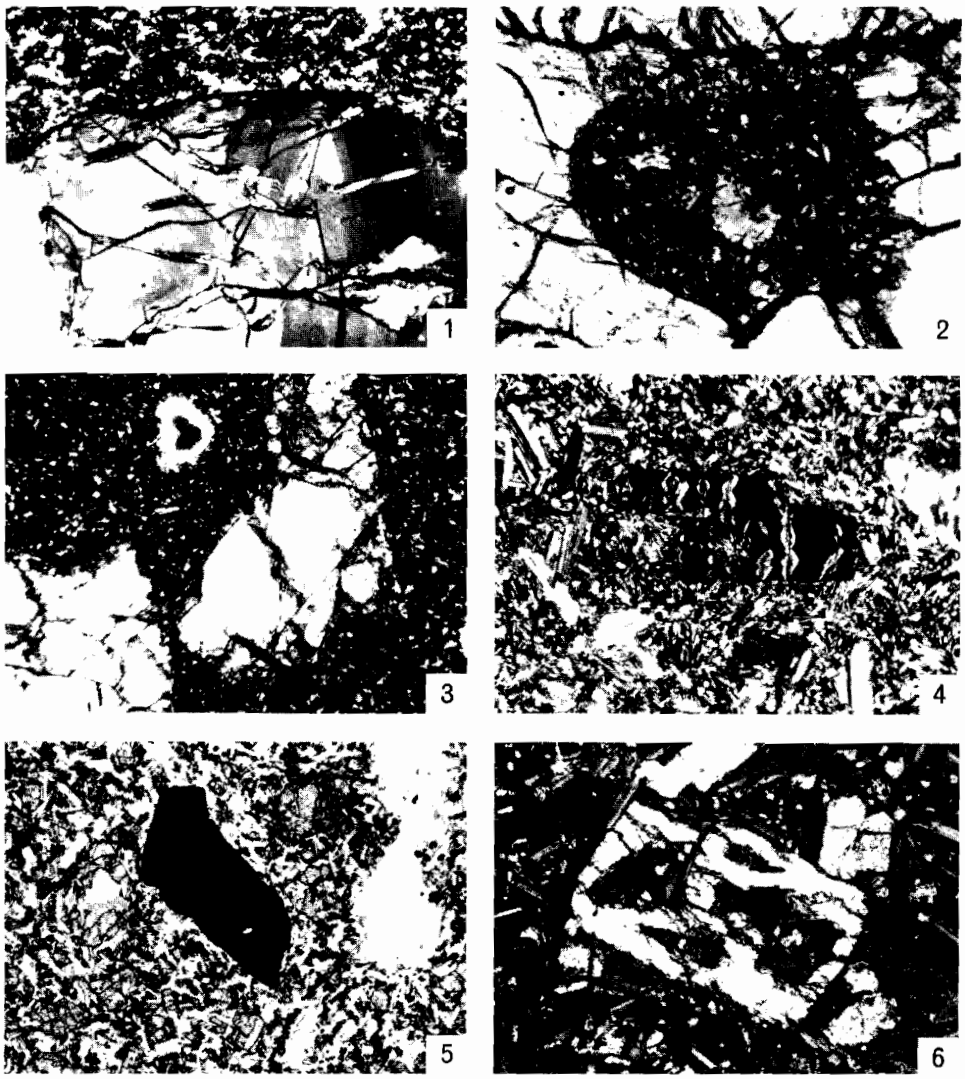


**Plate IV.** The enclosing basalt.

**Figure**

1 Basalt-lherzolite contact. PPL, ×8.
2 Basaltic infiltration nesting in the lherzolite inclusion. PPL, ×8.
3 Detached olivine fragment in amygdaloidal basalt. PPL, ×8.
4 Phlogopitised olivine xenocryst in basalt. Crossed polarisers, ×8.
5 Chrome-spinel xenocryst in basalt. PPL, ×13.
6 Idiomorphic tecoblastic olivine in basalt. Crossed polarisers, ×32.

basaltic fluids in the enclosed ultramafic bodies is printed in the deposition of basaltic nests within the xenoliths (Plate IV, Fig. 2). The avenues for these nests can be observed as trails in the fractured minerals and may appear as smears on mineral surfaces (Plate III, Fig. 5).

Fragmentation of the spinel-lherzolite xenoliths is quite apparent where stray fragments occur trapped in basaltic groundmass (Plate IV, Fig. 3). Olivine detached from the xenoliths can be easily identified microscopically by its twinning and phlogopitic alteration (Plate IV, Fig. 4). Some olivine crystals may develop kelyphitic rims. Similarly, a few chrome-spinel xenocrysts were also observed with magmatically corroded black margins (Plate IV, Fig. 5).

Genuine basaltic olivine occurs dispersed between the other basaltic minerals, plagioclase and augitic pyroxene. Tecoblastic olivine (Stanik 1970, cited in Augustithis 1978) tends to develop exerting its crystal boundaries on the groundmass minerals (Plate IV, Fig. 6). Basaltic olivines differ from the lherzolitic olivine in the absence of deformational twin lamellae and phlogopitisation. The modal composition of the enclosing basalt is shown in Table 1. It is interesting to note here that the basalt is partially contaminated by digesting some of the limestone xenoliths enclosed during the ascent of the lava. Surface weathering of this extremely hard and massive basalt is minimal. This is also extended to the trapped spinel-lherzolite xenoliths where fresh unweathered minerals can be safely studied. Basalt in contact with the xenoliths may include a bright green chlorite in the groundmass, which is most probably chromium-bearing and developed as an outcome of the magmatic corrosion of chrome-bearing diopside and spinel of the lherzolite inclusions.

## CHEMISTRY OF THE ULTRAMAFIC XENOLITHS

Chemical analysis of lherzolite xenoliths from Gebel Shihan and Gebel Aritain (north Jordan) is included in Table 2. The chemical analysis was done by XRF against USGS ultramafic standard rocks. The chemistry of the two analysed xenoliths are close, but the Shihan lherzolite is characteristically higher in $SiO_2$ and CaO content and lower in MgO content.

The relatively high $K_2O$ value for the Shihan lherzolite may be attributed to the phlogopitisation of generation I olivine. Obata & Thompson (1981) stressed the ultimate appearance of phlogopite in mantle ultramafic rocks with trace amounts of $K_2O$. They envisaged a biotite breakdown reaction involving a potassic (richterite) composition in the parent amphibole. The presence of pargasite or phlogopite in upper mantle lherzolite xenoliths is considered to reflect a metasomatic event in the mantle conditions (Girod *et al.* 1981).

The normative composition and the Fo/Hy ratio increases in the Aritain xenolith (Table 2).

## CHEMISTRY OF THE BASALTIC ROCKS

Three basaltic rocks were chemically analysed (Table 3): one representing the basalt enclosing the lherzolite xenoliths, the second is porphyritic basalt from the Shihan volcanic cone and the third representing the basaltic dyke (Al-Kharaza dolerite) exposed in the nearby area of Wadi Al-Karak (see Fig. 1).

The enclosing basalt is characteristically high in MgO content which is related to its

contamination with the forsterite fragments detached from the lherzolite xenoliths. The doubtful presence of nepheline in these basalts appeared in the normative composition. Part of the normative Fo is derived by contamination from the lherzolitic olivine.

The ferriferous nature of the porphyritic olivine basalt is well displayed in its chemical composition. Most of the $Fe_2O_3$ content is attributed to the surface alteration of olivine where hematitic dust occurs associated with the serpentine minerals. This may indicate that olivine of the enclosing basalts is more forsteritic than later formed basaltic flows. The slight increase in CaO content is due to the partial assimilation of Cretaceous limestone xenoliths.

**Table 2.** Chemical analysis and normative composition of the ultramafic xenoliths

| Chemical analysis | | | Normative composition | | |
|---|---|---|---|---|---|
| Oxide | Shihan | Aritain* | Mineral | Shihan | Aritain |
| $SiO_2$ | 45·950 | 42·380 | wo | 3·6 | 1·9 |
| $TiO_2$ | 0·090 | 0·050 | fs | 3·3 | 2·5 |
| $Al_2O_3$ | 1·700 | 2·040 | fo | 45·3 | 66·3 |
| $Fe_2O_3$ | 1·760 | 1·780 | mt | 1·7 | 1·6 |
| FeO | 6·210 | 6·520 | ap | — | 0·2 |
| MnO | 0·120 | 0·140 | hy | 41·8 | 22·0 |
| MgO | 40·770 | 44·280 | sp† | 4·3 | 5·5 |
| CaO | 2·000 | 1·080 | | | |
| $Na_2O$ | 0·006 | 0·006 | | | |
| $K_2O$ | 0·030 | 0·005 | | | |
| $P_2O_5$ | 0·070 | 0·140 | | | |
| $Cr_2O_3$ | 0·710 | 1·170 | | | |
| Total | 99·416 | 99·591 | | | |
| Ni(ppm) | 2156 | 2135 | | | |
| Cu (ppm) | 12 | 15 | | | |

* Ultramafic xenolith from the Aritain volcanic cone, north Jordan.

† Calculated as Fe $Al_2O_3$ + Fe $Cr_2O_3$.

The basaltic dyke of Wadi Al-Karak was analysed to characterise it chemically in order to test the possibility of regarding these dykes as feeders to the basaltic flows at Gebel Shihan. These rocks proved to contain more $SiO_2$ than the Shihan basalts and in the normative composition more hypersthene appeared in addition to quartz. These characteristics may favour a tholeiitic basaltic parentage for this dyke in contrast to the olivine basaltic nature of the Shihan basalt.

One is inclined to conclude that Shihan basalts with the lherzolite xenoliths erupted independently and that the dykes exposed in Al-Karak area (Al-Kharaza dolerites, Fig. 1) were intruded at a different time from that of Shihan volcano. The magmatic source is different in both cases.

**Table 3.** Chemical analysis and normative composition of some basaltic rocks

| | Chemical analysis | | | Normative composition | | | |
|---|---|---|---|---|---|---|---|
| Oxides | $B_1$ | $B_2$ | $B_3$ | Mineral | $B_1$ | $B_2$ | $B_3$ |
| $SiO_2$ | 45·20 | 44·80 | 49·45 | or | 6·5 | 5·5 | 6·5 |
| $TiO_2$ | 2·32 | 1·58 | 2·81 | ab | 18·3 | 29·0 | 27·0 |
| $Al_2O_3$ | 12·80 | 13·72 | 13·13 | an | 15·8 | 22·0 | 20·4 |
| $Fe_2O_3$ | 3·57 | 10·95 | 2·66 | ne | 8·7 | — | — |
| FeO | 7·68 | 2·04 | 8·80 | wo | 10·8 | 14·8 | 10·2 |
| MnO | 0·16 | 0·17 | 0·21 | fs | 6·4 | — | 8·0 |
| MgO | 11·35 | 7·60 | 6·50 | fo | 18·0 | 14·8 | — |
| CaO | 9·03 | 11·63 | 9·43 | mt | 3·3 | 1·5 | 3·0 |
| $Na_2O$ | 3·57 | 3·10 | 2·88 | il | 3·2 | 2·2 | 4·0 |
| $K_2O$ | 1·11 | 0·85 | 1·08 | ap | 0·8 | 0·5 | 1·3 |
| $P_2O_5$ | 0·41 | 0·36 | 0·61 | hy | 8·0 | 2·8 | 18·8 |
| $H_2O^-$ | 0·62 | 0·64 | 0·72 | hm | 0·2 | 6·9 | — |
| $H_2O^+$ | 2·16 | 2·74 | 1·40 | qz | — | — | 0·8 |
| Total | 99·98 | 100·18 | 99·68 | Pl(an+ab) | 34·1 | 51·0 | 47·4 |
| Cr (ppm) | 397 | 396 | 379 | | | | |
| Ni (ppm) | 225 | 188 | 58 | | | | |
| Cu (ppm) | 40 | 38 | 45 | | | | |

*Code:*

$B_1$: Hard black microporphyritic basalt, host to the lherzolite inclusions, Gebel Shihan.

$B_2$: Porphyritic olivine (serpentinised) basalt, Gebel Shihan.

$B_3$: Dolerite dyke, Al-Kharaza, Al-Karak.

## SUMMARY AND CONCLUSIONS

Quaternary alkali-olivine basaltic volcanic cones in Jordan could be regarded as targets for studying ultramafic xenoliths of possible mantle derivative. The ultramafic xenoliths of Gebel Shihan are mono-xenolithic and close to lherzolite in composition. The lherzolite xenoliths consist of forsterite, Fe-enstatite, chrome-diopside and chrome-spinel. The minerals are remarkably fresh, sealed by the fresh hard massive enclosing basalt. Serpentinisation of olivine is completely absent; so the study of the lherzolite minerals is not hampered by the extraneous effects. Two generations of the mineral constituents are observed and their textural relationships are important in understanding the environment under which these minerals have been formed.

The most interesting feature is the phlogopitisation of generation I olivine, where phlogopite occurs and is dusted with chrome-spinel. The xenoliths have been subjected to pressure which resulted in crushing of the individual minerals, especially olivine, and in the formation of prominent cataclastic textures. The enclosing basalts show reaction margins toward the xenoliths and are highly contaminated with the fragmented lherzolitic minerals.

Chemically, the lherzolite xenoliths are low in MgO and high in $SiO_2$ if compared with those of Gebel Aritain, north Jordan. Shihan basalts are undersaturated alkali olivine basalts while the basaltic dykes (dolerites) exposed in nearby areas are saturated

tholeiitic basalts. Lherzolite xenoliths are confined to the alkali olivine basalts in volcanic cones and are not found in the tholeiitic fissure eruption types.

Ultramafic xenoliths, so far recorded, are only known from young (Pleistocene-Recent) olivine basaltic rocks situated on the eastern side of the Red Sea–Dead Sea rift, and are unknown from the extensive Tertiary-Quaternary basaltic rocks of Egypt.

Ghent *et al.* (1980), related the diversity of the xenolithic inclusions, mafic and ultramafic, in Al-Birk alkaline olivine basalts in Saudi Arabia, to eruption in the thick Precambrian crust. On the other hand mono xenolithic inclusions (depleted harzburgites) occur in basalts which erupted through the thinner Miocene oceanic crust. The ultramafic xenoliths studied from the Shihan alkaline olivine basalts, fall within the lherzolite composition. The other inclusions are a few Cretaceous limestones, marginally heated and metamorphosed. Gabbroic xenoliths or Precambrian rock fragments were not found. It is possible to envisage that the sedimentary succession at Gebel Shihan (Cretaceous and older rocks) are underlain by a mafic-ultramafic layer and that the source of the ultramafic inclusions which are brought with the basaltic eruption is shallow.

On the basis of seismic data, Ginzburg & Makris (1979) proposed a crustal thinning toward Lake Tiberias and in the Dead Sea rift zone. Crustal thickness of the order of 30 km was proposed to characterise the Dead Sea graben.

The possible mantle derivative of the Shihan refractory spinel-lherzolite inclusions is not unlikely. They are texturally and mineralogically comparable to those described from other world occurrences. Derivation from unfractioned mantle is attributed to the depleted harzburgites recorded from basaltic rocks erupted through Red Sea coastal plain Miocene oceanic crust (Ghent *et al.* 1980). Spinel lherzolites recently described from the Island of Zabargad in the Red Sea were regarded by Bonatti *et al.* (1981) to be derived from the upper mantle at a depth of 30 km.

Considerable horizontal slickensiding has been recently observed by the author in Al-Karak area in extensive E–W faulted zones. The currently reputed E–W normal faults (Bender 1968; Hatcher *et al.* 1981) may prove to be transcurrent faults. In this respect, central volcano types such as Gebel Shihan volcanic cone should be associated with transcurrent rather than normal faulting.

## REFERENCES

**Augustithis, S.S. 1978.** Atlas of the textural patterns of basalts and their genetic significance. Elsevier, Amsterdam, 323 pp.

**Basta, E.Z. & Hanafy, M.A. 1970.** Alteration of some Egyptian chromites. Proc. Egypt. Acad. Sci. **23:** 1–7.

**Bender, F. 1968.** Geologie von Jorndanien. Gebruder Borntraeger, Berlin, 230 pp.

**Bonatti, E., Hamlyn, P. & Ottonello, G. 1981.** Upper mantle beneath a young oceanic rift: Peridotites from the island of Zabargad (Red Sea). Geology **9:** 474–79.

**Ghent, E.D., Coleman, R.G. & Hadley, D.G. 1980.** Ultramafic inclusions and host alkali olivine basalts of the southern coastal plain of the Red Sea, Saudi Arabia. Amer. J. Sci. **280-A:** 499–527.

**Ginzburg, A. & Makris, J. 1979.** Gravity and density distribution in the Dead Sea Rift and adjoining areas. Tectonophysics **54:** 17–25.

**Girod, M., Dautria, J.M. & Giovanni, R. de. 1981.** A first insight into the constituion of the upper mantle under the Hoggar area (southern Algeria): The lherzolite xenoliths in alkali basalts. Contrib. Mineral. Petrol. **77:** 66–73.

**Hatcher, R.D., Zietz, I., Regan, R.D. & Abu-Ajamieh, M. 1981.** Sinistral strike slip motion on the Dead Sea Rift: Confirmation from new magnetic data. Geology **9:** 458–62.

**Mercier, J.C.C. & Nicolas, A. 1975.** Textures and fabrics of upper-mantle peridotites as illustrated by xenoliths from basalts. J. Petrology **16:** 454–87.

**Obata, M. & Thompson, A.B. 1981.** Amphibole and chlorite in mafic and ultramafic rocks in the lower crust and upper mantle. Contrib. Mineral. Petrol. **77:** 74–81.

*(Received 21 April 1982)*

# تواجد فتات من صخور الليرزوليت في الصخور البازلتية بمنطقة شيحان ، الاردن

محمد عبد الحميد الشرقاوي
قسم الجيولوجيا بجامعة الكويت

## خلاصة

عند دراسة الصخور البركانية بالمخروط البركاني بمنطقة شيحان بوسط الاردن لوحظ وجود فتات من صخور الليرزوليت التى تحتوى على معدن الاسبينل محفوظة داخل الصخور البازلتية القلوية الصلدة . يشتمل التركيب المعدني لهذه الصخور على معادن الفورشتيريت والانستاتيت الحديدي والدايوبسيد الكرومي والاسبينل الكرومي مشكلين في نسيج بروتوجلانيولاري . وقد أمكن تمييز جيلين من المعادن مجهريا ، وتكون معادن الجيل الأول صغيرة وغالبا محتواة داخل معادن الجيل الثاني الكبيرة . يتكون الفلوجوبيت من تحلل معدن الفورشتيريت التابع للجيل الأول . تزدحم الصخور البازلتية بالمعادن المهشمة الناتجة من تكسر وتفكك مكونات فتات صخور الليرزوليت مما يؤثر على تركيبها المعدني الكيميائي . وبدراسة التداخلات الدوليريتية المتكشفة في الاماكن المجاورة لمنطقة شيحان اتضح انها ليست المصدر للطفوح البازلتية بالمنطقة المدروسة وذلك نظرا لانها ذات أصل ثولييتي بالمقارنة بالاصل البازلتي القلوي لصخور شيحان .

من المحتمل ان يكون مصدر فتات صخور الليرزوليت المتواجدة بصخور بازلت شيحان هو الغطاء العلوي داخل الأرض ، كما ان البراكين المتمركزة التى تشبه بركان شيحان قد تصاحب فوالق ذات ازاحة جانبية مضربية قاطعة بدلا من الفوالق العادية . ومن هذه الدراسة يمكن استنتاج ان الصخور البركانية القلوية الحديثة بالاردن والاماكن المجاورة بالسعودية وسوريا ستكون قريبة الشبه بتلك الموجودة في شيحان . وبالفعل ففي شمال الاردن وجدت كميات كبيرة من فتات من صخور الليرزوليت في بركان الرئتين ، تماثل ما وجد في منطقة شيحان بوسط الاردن .